Glycosylated Peptide Hormones: Pharmacological Properties and Conformational Studies of Analogues of [1-Desamino,8-D-arginine]vasopressin

Jan Kihlberg* and Jens Åhman

Organic Chemistry 2, Chemical Center, The Lund Institute of Technology, University of Lund, P.O. Box 124, S-221 00 Lund, Sweden

Björn Walse and Torbjörn Drakenberg

Physical Chemistry 2, Chemical Center, The Lund Institute of Technology, University of Lund, P.O. Box 124, S-221 00 Lund, Sweden

Anders Nilsson, Christina Söderberg-Ahlm, Bengt Bengtsson, and Håkan Olsson*

FERRING Research Institute AB, P.O. Box 30047, S-200 61 Malmö, Sweden

Received July 18, 1994[⊗]

Two analogues of the antidiuretic drug [1-desamino,8-D-arginine]vasopressin (DDAVP), which have a glycosylated serine at position 4, have been prepared by Fmoc solid phase peptide synthesis. The glycosylated analogues had significantly higher bioavailabilities than the nonglycosylated [D-Tyr^2,Ser^4]DDAVP and DDAVP on intraintestinal administration in rat. The improved bioavailability resulted from an increased absorption from the small intestine and most likely from an increased stability toward enzymatic degradation, whereas plasma clearance was either unaffected or slightly increased by the glycosylation. The glycosylated analogues displayed only very low agonistic and antagonistic activities at the vasopressin V_2-receptor. Conformational studies performed by ^{1}H NMR spectroscopy did not reveal any major influence from glycosylation on the conformation of the peptide backbone. The lack of receptor binding displayed by the analogues is therefore most likely explained by steric repulsion between the carbohydrate moiety and the vasopressin receptor which prevents receptor binding.

Introduction

The oligosaccharide units of naturally occurring glycoproteins are known to affect the properties of the parent protein in many and diverse ways (reviewed in refs 1 and 2). For example, glycosylation of a protein can confer protection against proteolysis, influence uptake, distribution, and excretion, and it can also determine the biological function of the protein. These effects can in some cases be indirect consequences of the glycosylation which result from conformational changes induced in the protein by the carbohydrate moieties.

Some recent investigations have revealed that attachment of carbohydrate residues to peptides, which are not glycosylated in nature, can influence the biological functions of the peptides as enzyme inhibitors, neuropeptides, and hormones. For instance, a glycosylated derivative of a peptide inhibitor of the protease renin displayed slower excretion by the liver biliary pathway than the parent peptide, resulting in increased serum availability.[3] Several neuropeptides and peptide hormones have been glycosylated, and strikingly, the analgetic (antinociceptive) activity of [D-Met^2,Hyp^5]-enkephalinamide was increased 200–2000-fold on β-D-galactosylation of the hydroxyproline.[4] In addition, a recent communication[5] describes that attachment of glucose to an enkephalin analogue enables the neuropeptide to cross the blood–brain barrier, presumably via an active glucose transport mechanism. Smaller increases, or decreases, in the biological activity were also observed on glycosylation of other enkephalin analogues[6,7] and of analogues of somatostatin,[8] LHRH,[9] and vespulakinin.[10] These studies illustrate that glycosylation can be used as a tool to modify the biological activities of peptides. In addition, a few studies indicate that glycosylation can be exploited in attempts to overcome the intrinsic shortcomings in using peptides as drugs,[11] i.e., to overcome rapid excretion,[3] poor transport across membranes such as the blood–brain barrier,[5] and susceptibility to proteolytic degradation.[12]

We have prepared the two glycosylated analogues **6** and **7** of the antidiuretic drug DDAVP, [1-desamino,8-D-arginine]vasopressin[13] (**4**), as well as the nonglycosylated analogue **5**. The glycopeptides were prepared in order to investigate if glycosylation could improve the metabolic stability and the uptake of DDAVP on intraintestinal administration and also to determine its effect on the antidiuretic activity of DDAVP and on the conformation of the peptide backbone. We replaced glutamine at position 4 in DDAVP by a galactosylated serine, since various amino acids including serine can be incorporated at this position without loss of the antidiuretic activity.[14] The Tyr^2-Phe^3 and Phe^3-Gln^4 amide bonds in DDAVP are labile toward proteolysis by α-chymotrypsin, but use of D-Tyr at position 2 stabilizes the former bond toward cleavage with only a minor reduction[14] of the antidiuretic activity. D-Tyr^2 was therefore incorporated in **5**–**7** in order to allow an evaluation of the influence of glycosylation on the stability of the Phe^3-Ser^4 amide bond toward enzymatic degradation.

[⊗] Abstract published in *Advance ACS Abstracts*, December 1, 1994.

0022-2623/95/1838-0161$09.00/0

Scheme 1

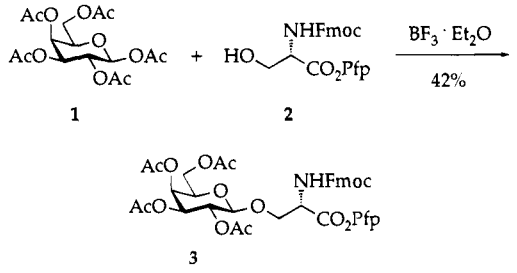

Mpr-**AA1**-Phe-**AA2**-Asn-Cys-Pro-D-Arg-Gly-NH_2

(Mpr = 3-mercaptopropionic acid)

4 AA1 = L-Tyr, AA2 = Gln

5 AA1 = D-Tyr, AA2 = Ser

6 AA1 = D-Tyr, AA2 = 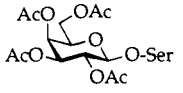

7 AA1 = D-Tyr, AA2 = 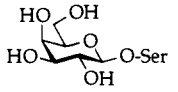

Results and Discussion

Glycopeptide Synthesis. The glycosylated building block **3** was obtained (42%) by boron trifluoride etherate promoted glycosylation[15] of N^{α}-Fmoc-L-serine pentafluorophenyl ester[16] (**2**) with β-D-galactose pentaacetate (**1**) (Scheme 1). Compound **3** was then used for synthesis of the glycosylated DDAVP analogues **6** and **7** according to standard conditions for Fmoc solid phase peptide synthesis. The synthesis was performed in a mechanically agitated reactor on a polystyrene resin functionalized with the Rink linker,[17,18] and N^{α}-Fmoc amino acids carrying standard side chain protective groups were coupled to the resin as benzotriazolyl (HOBt) esters.[19] After completion of the synthesis, the glycopeptides were cleaved from the resin, and the amino acid side chains were simultaneously deprotected by treatment with trifluoroacetic acid. Disulfide bond formation was affected by oxidation with iodine in methanol. In the preparation of **7** it was found that deacetylation had to precede disulfide bond formation since the cyclized glycopeptide **6** was degraded on attempted deacetylation with methanolic ammonia. Purification by reversed phase HPLC gave the glycopeptides **6** and **7** in 30 and 20% overall yields, respectively, based on the resin capacity. The nonglycosylated DDAVP analogue **5** was prepared by a similar procedure in 44% yield. The glycopeptides were characterized by fast atom bombardment mass spectrometry, amino acid analysis, and ^{1}H NMR spectroscopy.

Biochemical and Pharmacological Studies. The influence of glycosylation on susceptibility toward proteolytic degradation, uptake on intraintestinal administration, and the antidiuretic activity of DDAVP (**4**) was investigated in comparative studies using the analogues **5**–**7**.

Table 1. Degradation of DDAVP (**4**) and **5**–**7** *in Vitro* by α-Chymotrypsin and Rat Intestinal Juice[a]

	$t_{1/2}$ (min)	
peptide	α-chymotrypsin	rat intestinal juice
4	13 ± 1	20 ± 1
5	37 ± 2	280 ± 30
6	180 ± 5	230 ± 10
7	37 ± 1	320 ± 30

[a] Half-lives were calculated from the time-course studies of degradation using the formula for single exponential decay. Results are from one experiment and are expressed ± SE of the calculated half-life.

Table 2. Transport Rates of DDAVP (**4**) and **5**–**7** *in Vitro* over Rat Small Intestine[a]

		relative transport rate	
peptide	transport rate P_{app} (×10^6, cm/s)	P_{app}(peptide)/ P_{app}(PEG 1000)	P_{app}(peptide)/ P_{app}(PEG 4000)
4 (n = 6)	0.89 ± 0.06	0.57 ± 0.03	1.57 ± 0.08
5 (n = 4)	1.03 ± 0.06	0.62 ± 0.05	1.66 ± 0.14
6 (n = 4)	1.84 ± 0.11	1.09 ± 0.03	2.83 ± 0.11
7 (n = 4)	1.67 ± 0.08	0.96 ± 0.03	2.56 ± 0.07

[a] Values are mean ± SEM calculated from transport rates of nine 15-min intervals of n individual experiments

First, the stability of the peptides **5**–**7** toward proteolytic degradation by α-chymotrypsin and rat intestinal juice was investigated with DDAVP as reference (Table 1). A 3-fold increase in half-life was observed for **5** and the glycosylated **7** in the degradation with chymotrypsin, whereas the *O*-acetylated glycopeptide **6** displayed a more than 10-fold higher stability. The general increase in stability of **5**–**7** is most likely due to the incorporation of D-Tyr at position 2, which stabilizes the Tyr^2-Phe^3 amide bond, whereas the additional stability of **6** must result from stabilization of the Phe^3-Ser^4 bond by the bulky *O*-acetylated galactose moiety. In contrast, compounds **5**–**7** all displayed similar rates of degradation by rat intestinal juice, and their half-lives increased 10–15-fold in comparison to DDAVP. Again, the increase in stability most certainly results from incorporation of D-Tyr at position 2, but with the complex enzymatic mixture which constitutes rat intestinal juice, no pronounced increase in the stability due to the glycosylation was observed.

Peptides generally display poor absorption on oral administration, and only approximately 0.1% of the administered dose of DDAVP is absorbed in humans[20] and in rat (Table 3). The uptake of DDAVP, and the peptides **5**–**7**, over rat small intestine was assessed by measuring the transport rates over a segment of small intestine mounted in a modified Ussing chamber. The absence of enzymatic degradation in this experiment was verified by incubating DDAVP, the peptide shown to be most susceptible to degradation, with a piece of intestine and analyzing the DDAVP concentration by radioimmunoassay and HPLC. The glycopeptides **6** and **7** were transported across the small intestine at higher rates than the nonglycosylated **5** and DDAVP, with the *O*-acetylated glycopeptide **6** showing the highest transport rate (P_{app}, Table 2). Small but noticeable differences in transport rates were evident between the experiments due to individual variation in intestine from different rats. The radiolabeled poly(ethylene glycols) [^{3}H]PEG 1000 and [^{14}C]PEG 4000 were therefore included as internal control substances to allow correction of inter individual variation. The relative

Table 3. Some Pharmacokinetic Parameters of DDAVP (**4**) and **5**–**7** after Intravenous and Intraintestinal Administration to Rats[a,b]

	intravenous (iv)		intraintestinal (ii)		
peptide	$t_{1/2}$[c] (min)	AUC[d] (ng/mL·min)	C_{max}[e] (ng/mL)	AUC[d] (ng/mL·min)	bioavailability[f] (%)
4	39 ± 2 (3)	459 ± 18 (3)	0.8 ± 0.1 (4)	52 ± 9 (4)	0.1
5	32 ± 1 (4)	278 ± 18 (4)	1.4 ± 0.3 (4)	141 ± 50 (4)	0.5
6	35 ± 2 (4)	298 ± 17 (4)	3.6 ± 0.5 (4)	620 ± 77 (4)	2.1
7	20 ± 2 (4)	211 ± 25 (4)	2.5 ± 1.3 (4)	345 ± 102 (4)	1.6

[a] Of each peptide, 1 μg was administered intravenously and 100 μg was administered intraintestinally. [b] Values are mean ± SEM of n individual experiments. [c] Half-life. [d] Area under plasma concentration curve. [e] Maximal concentration in plasma. [f] The bioavailability was calculated as $(AUC_{ii}/dose_{ii})/(AUC_{iv}/dose_{iv})$.

transport rates showed that the glycopeptides **6** and **7** were transported to the serosal side of the small intestine at approximately the same rate as PEG 1000 and almost three times the rate of the larger PEG 4000 (Table 2). In contrast, the peptide **5** and DDAVP were transported at only half the rate of PEG 1000 and 50% faster than PEG 4000. The tetra-*O*-acetylated glycopeptide **6** displayed somewhat higher relative transport rates than the deprotected glycopeptide **7** both in relation to PEG 1000 and PEG 4000.

DDAVP and the three peptides **5**–**7** all showed the same biphasic elimination pattern after intravenous (iv) administration in the rat, the first phase representing distribution combined with elimination and the second phase representing only elimination (data not shown). The elimination rate during the second phase followed single exponential decay for all four peptides, and the kinetic analysis after iv administration demonstrated that the half-lives of the nonglycosylated **5** and the *O*-acetylated glycopeptide **6** were in the same range as DDAVP, while the deprotected **7** showed a considerably higher rate of clearance (Table 3). As expected, the AUC (area under plasma concentration curve) values ranked the four peptides in the same order as did the half-lives (DDAVP > **6** > **5** > **7**). Since the hydrophilic DDAVP is known to be predominantly excreted via the kidneys, a possible explanation for the enhanced clearance of **7** may be that incorporation of a hydrophilic, unprotected carbohydrate moiety facilitates the excretion. Another explanation could be that the carbohydrate residue enables the substance to be cleared via an additional route.

The absorption *in vivo* from rinsed rat intestine differed markedly between the peptides. The glycopeptides **6** and **7** displayed higher maximal plasma concentrations (C_{max}), reflecting faster and more efficient absorption than the peptide **5** and DDAVP (Figure 1 and Table 3). Furthermore, the two glycopeptides displayed time to maximum concentration values (t_{max}) between 30 and 60 min in contrast to **5** and DDAVP, which both reached their maximal concentrations within 15 min (Figure 1). The higher C_{max} and increased t_{max} suggest that **6** and **7** were available for transport from the intestine during a longer period of time than **5** and DDAVP. This indicates a higher stability of **6** and **7** toward enzymatic degradation in the intestine and possibly also in the intestinal wall. The bioavailability of the peptides, calculated by comparing the AUC values from intraintestinal administration with AUC values from intravenous administration, clearly demonstrated a considerably higher bioavailability for the glycosylated peptides (Table 3). The *O*-acetylated glycopeptide **6** was the most bioavailable, displaying a 4-fold increase in bioavailability in comparison to **5** and a 20-fold increase in comparison to DDAVP.

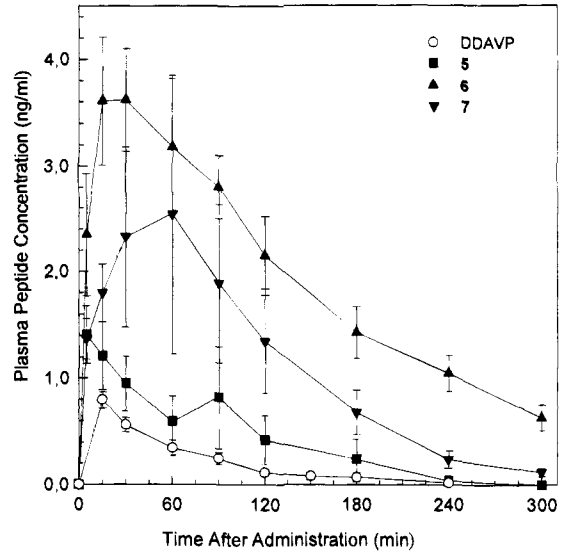

Figure 1. Plasma concentrations of DDAVP (**4**) and the analogues **5**–**7** after intraintestinal administration to anaesthetized rats; 100 μg of each peptide was administered into the rat intestine, and the plasma peptide concentration was determined at the indicated time points by radioimmunoassay. The data are means ± SEM (n = 4).

The increase in bioavailability of the glycosylated **6** and **7**, as compared to **5** and DDAVP, is most likely a result of the combined effects of glycosylation and inversion of configuration at Tyr[2] on absorption, degradation, and excretion. The 2-fold increase in transport rate over rat small intestine observed for **6** and **7** *in vitro* illustrates the important influence played by glycosylation for the bioavailability, but the increased transport rate does not by itself account for the full increase in bioavailability. An additional effect is likely to come from a higher stability of the glycosylated **6** and **7** toward degradation in the intestinal wall and mucosa and also in the plasma. The recent observation[12] that glycosylation protects short peptides from proteolysis by human plasma and serum, and the observed increase in the stability of **6** toward chymotrysin, supports this hypothesis. The half-lives of DDAVP and **5**–**7** on intravenous administration reveal that glycosylation either does not significantly affect, or slightly increases the plasma clearance of DDAVP, thereby making no contribution to, or even decreasing, the bioavailability. In contrast to our results, Fisher and co-workers found[3] that glycosylation significantly decreased the rate of excretion of a peptide inhibitor of the aspartyl protease renin. The difference between the two observations may be explained by the fact that the hydrophilic peptides in our study are predominantly excreted via the kid-

Table 4. Vasopressin Receptor Agonistic and Antagonistic Properties *in Vivo* of DDAVP (**4**) and **5**–**7**

peptide	antidiuretic activity[a] (IU/μmol)	anti-antidiuretic activity[b] (% inhibition)
4	1130[c]	
5	810 ± 180 (5)	
6	0.31 ± 0.05 (4)	3 (2)
7	0.06 ± 0.01 (8)	4 (2)

[a] The antidiuretic activity was calculated using an international vasopressin standard (500 IU/μmol). Values are mean ± SEM of *n* individual experiments. [b] The anti-antidiuretic activity was calculated at 330-fold molar excess of **6** and **7** as percent inhibition of the antidiuretic effect of a fixed dose of vasopressin. Values are means of two individual experiments. [c] Fixed international standard value.

neys, whereas the hydrophobic renin inhibitor is largely excreted via the efficient liver biliary pathway. In the case of the renin inhibitor, addition of a hydrophilic carbohydrate moiety diverts clearance from the rapid liver biliary pathway to the slower renal pathway.[3]

The glycosylated DDAVP analogues **6** and **7** showed only minute antidiuretic activity on intravenous administration in rat, in contrast to the nonglycosylated **5** which retained approximately 70% of the antidiuretic activity of DDAVP (Table 4). Furthermore, the analogues **6** and **7** were extremely weak vasopressin receptor antagonists when evaluated with respect to the anti-antidiuretic effect *in vivo* in rats or *in vitro* in a receptor binding assay. In the *in vivo* studies, administration of a 330-fold excess of **6** and **7** over vasopressin resulted in only a <5% inhibition of the antidiuretic V_2-receptor response (Table 4). *In vitro*, a 10 000-fold molar excess of **6** and **7** displaced 45 and 55% of the [^{3}H]vasopressin from the receptor, in the absence as well as in the presence of the V_1-antagonist [Phenylac^1,D-Tyr(Me)^2,-Arg^{6,8},Lys-NH$_2$^{9}]vasopressin, indicating a very weak binding of **6** and **7** to both the V_1- and the V_2-receptor. This lack of both antidiuretic and vasopressin antagonistic activity demonstrates that a glycosylated serine cannot be incorporated at position 4 in DDAVP with retained receptor binding activity, although serine as well as other amino acids can be successfully accommodated at this position.

Conformational Studies. The lack of receptor binding displayed by the glycopeptides **6** and **7** can be due to either steric interference between the carbohydrate moiety and the vasopressin receptor, or to an influence from the carbohydrate moiety on the conformations which can be adopted by the peptide part. In an attempt to further investigate these alternatives, we studied the differences in conformations between DDAVP and **6** and **7** using ^{1}H NMR spectroscopy.

We have recently performed a study of the conformations of DDAVP (**4**) in aqueous solution in which data from ^{1}H NMR spectroscopy was used to obtain three-dimensional structures by a combination of distance geometry calculations and simulated annealing.[21] The calculations gave two main conformational families for DDAVP, and the lowest energy conformation which belongs to the largest family is shown in Figure 2. All the calculated conformations were highly similar in the macrocyclic hexapeptide ring and displayed an inverse γ-turn around Gln^4 with a hydrogen bond between Phe^3 C=O and Asn^5 N–H. Only the backbone dihedral angles for Tyr^2 and Phe^3 differed significantly between the two main conformational families. The crystal

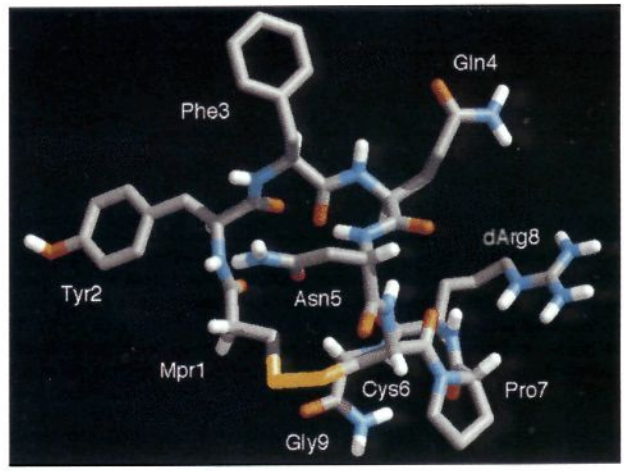

Figure 2. The lowest energy conformation of DDAVP (**4**) in aqueous solution as determined by NMR spectroscopy and conformational calculations.[21] The glycopeptides **6** and **7** were shown to assume similar conformations after taking the configurational change at Tyr^2 and the replacement of Gln^4 by a glycosylated Ser into account. Hydrogen atoms attached to side chain carbon atoms have been omitted for clarity. (The figure was generated using the software MidasPlus from UCSF, USA.)

structure[22] of pressinoic acid (the macrocyclic moiety of vasopressin) displays type II′ and type I β-turns centered around Phe^3-Gln^4 and Gln^4-Asn^5, respectively. In DMSO solution, NMR studies indicated a β-turn at the Phe^3-Gln^4 residues of arginine vasopressin and analogues.[23,24] We found that the largest conformational family for DDAVP lacks such β-turns in the macrocyclic ring, whereas the other family has retained a somewhat distorted Phe^3-Gln^4 type II′ β-turn. A common characteristic for all the calculated conformations is that the aromatic side chains of Tyr^2 and Phe^3 are directed away from the ring and the side chain of Asn^5 stretches over the top of the ring toward Tyr^2 (Figure 2). The calculated conformations all differ in the disulfide moiety and also for residues Pro^7-Gly^9, which make up the exocyclic tail. The former observation may be due to a lack of useful NOE's, whereas the latter indicates flexibility.

^{1}H NMR spectroscopy revealed differences both in chemical shifts (Table 5 and Figure 3) and nuclear Overhauser enhancements (NOE's, Figure 4) between DDAVP and the glycosylated analogues **6** and **7**. As discussed in greater detail below, most of the differences in chemical shifts and NOE's could be accounted for by the structural differences between DDAVP and **6** and **7**, i.e., the inverted configuration of Tyr^2 and introduction of a glycosylated Ser at position 4. In this analysis the observed spectroscopic differences could best be explained when interpreted using the largest conformational family of DDAVP,[21] represented by the lowest energy conformation (Figure 2). Since only minor differences in NMR data between DDAVP and **6** and **7** remained after taking the structural differences into account, we did not consider it necessary to develop the conformations of the glycosylated **6** and **7** independently from their own NMR data. Unfortunately, peptide **5** gave a viscous aqueous solution and could therefore not be investigated by NMR spectroscopy due to severe line broadening.

An upfield shift was observed for Tyr^2 H-α in the glycopeptides **6** and **7**, as compared to DDAVP (Figure

Table 5. ^{1}H NMR Chemical Shifts[a] (δ, ppm) in Water Containing 10% D_2O for DDAVP (**4**) and the Peptide Parts of Glycopeptides **6**[b] and **7**[b]

position	amino acid	proton	4[c]	6	7
1	Mpr[d]	α	3.15, 2.86	2.98, 2.90	2.95, 2.87
		β	2.60[e]	2.79, 2.52	2.77, 2.51
2	Tyr[f]	NH	8.28	8.59	8.58
		α	4.56	4.39	4.40
		β	2.95, 2.66	3.01, 2.69	2.98, 2.72
		arom[g]	6.97, 6.77	7.04, 6.79	7.04, 6.79
3	Phe	NH	7.76	7.73	7.81
		α	4.67	4.75	4.76
		β	3.36, 3.01	3.25, 2.86	3.26, 2.87
		arom[h]	7.40, 7.34	7.35, 7.31	7.32, 7.29
			7.27	7.21	7.16
4	Ser	NH		8.62	8.53
		α		4.41	4.54
		β		4.11, 3.99	4.21, 3.92
	Gln	NH	8.53		
		α	4.07		
		β	2.08[e]		
		γ	2.28[e]		
		γ-$CONH_2$	7.62, 6.95		
5	Asn	NH	8.27	8.06	8.28
		α	4.69	4.75	4.71
		β	2.86, 2.77	2.76[e]	2.76[e]
		β-$CONH_2$	7.68, 6.92	7.69, 6.92	7.68, 6.99
6	Cys	NH	8.19	8.48	8.60
		α	4.82	–[i]	4.93
		β	3.09, 2.91	3.17, 2.71	3.15, 2.69
7	Pro	α	4.43	4.46	4.46
		β	2.30, 1.92	2.33, 1.93	2.31, 1.93
		γ	2.06[e]	2.05[e]	2.06[e]
		δ	3.84, 3.71	3.86, 3.72	3.86, 3.72
8	D-Arg	NH	8.83	8.85	8.84
		α	4.29	4.32	4.31
		β	1.93, 1.77	1.93, 1.76	1.93, 1.77
		γ	1.64[e]	1.64[e]	1.64[e]
		δ	3.19[e]	3.21[e]	3.20[e]
		δ-NH	7.26	7.27	7.26
9	Gly	NH	8.44	8.47	8.47
		δ	3.89[e]	3.90[e]	3.91[e]
		α-$CONH_2$	7.38, 7.20	7.44, 7.20	7.45, 7.21

[a] Obtained at 500.13 MHz, 278 K, and pH = 5.65 with H_2O (δ_H 4.98) as internal standard. Chemical shifts are accurate to ±0.02 ppm. [b] ^{1}H NMR chemical shifts (δ, ppm) for the galactose moiety in **6**: 4.91 (H-1), 5.11 (H-2), 5.26 (H-3), 5.50 (H-4), 4.26 (H-5), 4.29[e] (H-6,6′) and **7**: 4.39 (H-1), 3.54 (H-2), 3.64 (H-3), 3.92 (H-4), 3.70 (H-5), 3.78 (H-6,6′). [c] Cf. ref 21. [d] Mpr = 3-mercaptopropionic acid. [e] Degeneracy has been assumed. [f] L-Tyr for **4**, D-Tyr for **6** and **7**. [g] Chemical shifts for the 2,6- and 3,5-protons, respectively. [h] Chemical shifts for the 3,5-, 4-, and 2,6-protons, respectively. [i] Resonance not seen due to water presaturation.

3), and can be explained as a result of the inversion of configuration at Tyr^2 (L-Tyr in DDAVP, D-Tyr in **6** and **7**). In DDAVP, Tyr^2 H-α is deshielded by close contacts with the carbonyl oxygen atoms of Mpr^1 and Tyr^2 (Figure 2), but the distances to these oxygen atoms increase by 1 Å or more when the configuration at Tyr^2 is inverted. Simultaneously, the distance between Tyr^2 H-α and Phe^3 N–H decreases, and an increase in the NOE between these protons was also observed for **6** and **7**. In addition, an increased NOE between Tyr^2 N–H and Phe^3 N–H was observed for **6** and **7**, corresponding to a decrease by more than 0.5 Å in the distance between these protons. This reveals a slight rotation of Phe^3 N–H toward Tyr^2 N–H in **6** and **7**, which also results in an increased intraresidue Phe^3 N–H → H-α distance, as revealed by the corresponding NOE. The inversion of configuration positions the aromatic side chain of Tyr^2 below the macrocyclic ring. This probably allows the C=O in the side chain of Asn^5 to come closer to Tyr^2 N–H (cf. Figure 2) and may explain the observed 0.3 ppm downfield shift of Tyr^2 N–H in **6** and **7**. Alternatively, this downfield shift may be caused by the change in the position of the aromatic ring of Tyr^2.

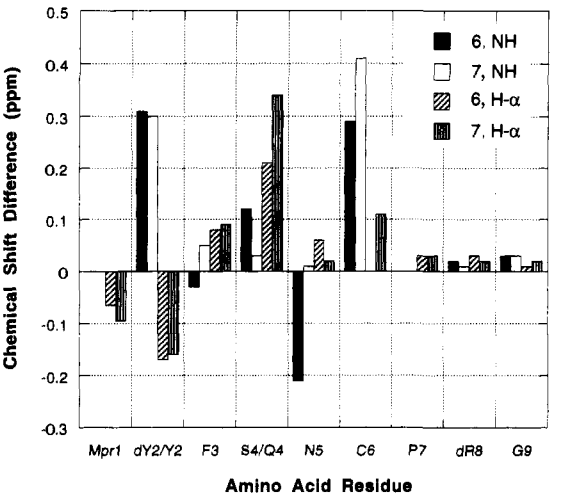

Figure 3. Differences in backbone NH and H-α NMR chemical shifts for each residue in the glycopeptides **6** and **7**, as compared to the corresponding residues in DDAVP (**4**). A positive difference indicates a downfield shift. The shift differences at position 4 have been corrected for the change in amino acids using the random coil chemical shift differences[42] between Gln and Ser (+ 0.03 ppm for the NH shift and −0.13 ppm for the H-α shift).

The downfield shift of Ser^4 H-α in **6** and **7** is due to the exchange of amino acids at this position (which has been compensated for in Figure 3, but not in Table 5) and to the substitution effect of the galactosyl residue attached to Ser^4. Similar substitution effects (0.15–0.26 ppm) have been reported previously on glycosylation of Ser in a T cell stimulating peptide[25] and of Ser and Thr in peptide analogues of human insulin-like growth factor 1.[26]

The calculated lowest energy conformation[21] for DDAVP displays a hydrogen bond between Cys^6 N–H and Gln^4 C=O. A downfield shift (0.3–0.4 ppm) was observed for Cys^6 N–H in **6** and **7** (Figure 3), indicative of an increase in the strength of this hydrogen bond. Cys^6 N–H also showed an increase in the NOE to Asn^5 H-α and a decrease in the NOE to Ser^4 H-α and Asn^5 N–H. Formation of a stronger hydrogen bond, i.e., a decrease in the N–*H* to C=*O* distance, can be obtained by a slight rotation of the backbone between Asn^5 and Cys^6, in the lowest energy conformation of DDAVP. Such a rotation results in a decrease in the distance from Cys^6 N–H to Asn^5 H-α and a concomitant increase in the distance to Ser^4 H-α and Asn^5 N–H, in agreement with the observed changes in NOE's. The conformational change may be due to either the amino acid substitution at position 4, or to the glycosylation at this position. The two alternatives can at present not be distinguished since the nonglycosylated analogue **5** could not be used for NMR studies due to the severe line broadening.

The NOE differences in the Pro^7-Gly^9 tail are difficult to probe due to the conformational flexibility found for the tail in DDAVP.[21] Furthermore the magnitude of some of the involved NOE's are uncertain due to their closeness to the water resonance.

Hydrophobic interactions between aromatic amino acid side chains and nonpolar faces of carbohydrates

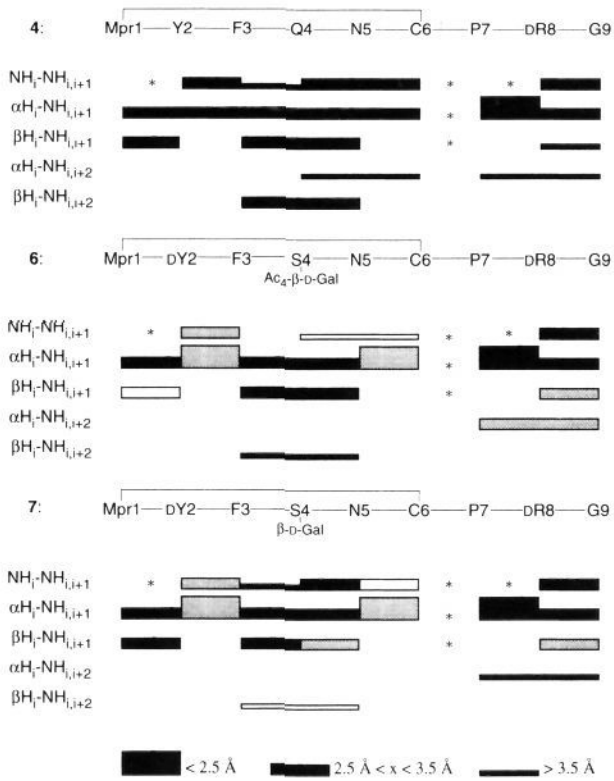

Figure 4. Schematic representation of interproton distances, as revealed by interresidue NOE connectivities, for DDAVP (**4**) and the glycopeptides **6** and **7**. The thickness of the lines indicate the length of the corresponding interproton distances as specified in the figure. For **6** and **7** a gray line indicates an interproton distance which is shorter, and a white line one that is longer, than the corresponding distance in DDAVP. The distance comparison is based upon the exact distances from integration of NOE's in the ROESY spectra, and the color marking reveals a distance differing by more than 0.2 Å. In cases where the line could contain two distances (e.g., $\beta H_i - NH_{i,i+1}$) the mean distance is showed. An asterisk (*) indicates an interproton distance which is nonexistant due to the absence of an amide proton.

have been shown to provide stabilization for complexes between antibodies and their carbohydrate ligands.[27,28] In the neoglycopeptides **6** and **7**, the side chains of Tyr^2 and Phe^3 could contact the Ser^4 galactosyl residue which displays a hydrophobic face made up of H-1,-3,-4 and H-5. No NOE's were observed between the galactose residue and the two aromatic side chains, and therefore such hydrophobic interactions do not seem to play a major role for the conformation adopted by glycopeptides **6** and **7**. It should be pointed out that it is also possible that the lack of NOE's results from a high flexibility for these three residues.

Most of the chemical shift and NOE differences observed on comparison of the glycopeptides **6** and **7** with DDAVP can thus be accounted for in terms of the structural changes, i.e., the inversion of configuration at Tyr^2 and the replacement of Gln^4 by a glycosylated Ser. Therefore the carbohydrate moiety in **6** and **7** has no, or only a minor, influence on the conformation adopted by **6** and **7** in aqueous solution. This is in agreement with previous studies of glycopeptides performed by us,[25] and others.[26,29,30] In contrast, reports[31,32] which describe a significant conformational influence from glycosylation have also been presented, illustrating that no general conclusions regarding conformational changes caused by glycosylation of peptides can be drawn.

The similar conformational preferences displayed by DDAVP and the glycosylated analogues **6** and **7** suggest that their lack of binding to the vasopressin receptor is most likely due to steric repulsions between the carbohydrate moieties and the receptor. Even though the conformational investigation does not reveal any major influence from the carbohydrate moiety on the conformations adopted by the peptide backbone in **6** or **7**, it cannot be entirely ruled out that the glycopeptides are unable to undergo conformational changes which might be necessary for binding to the vasopressin receptor.

Conclusions. The glycosylated DDAVP analogues **6** and **7** displayed significantly higher bioavailabilities than the nonglycosylated **5** and DDAVP on intraintestinal administration in rat. To the best of our knowledge this is the first report describing that attachment of a carbohydrate moiety to a peptide results in an increased bioavailability on intraintestinal administration. In part the improved bioavailability can be explained by an increased transport rate over rat small intestine. In addition, it is also most likely due to an increased stability of **6** and **7** toward enzymatic degradation in the intestine, the intestinal wall, and the plasma, induced by the carbohydrate moiety. Plasma clearance was found to be either unaffected or slightly increased by the glycosylation. The glycopeptides **6** and **7**, in contrast to the nonglycosylated **5**, did not display any antidiuretic activity, and **6** and **7** were also very weak vasopressin antagonists. Conformational studies revealed that DDAVP, and the glycosylated analogues, adopted similar conformations in aqueous solution, suggesting that the lack of receptor binding activity was most likely caused by steric hindrance between the carbohydrate moiety of **6** and **7** and the vasopressin receptor. Even though the conformational studies did not show any influence from the glycosylation on the conformations adopted by the peptide backbone of **6** and **7**, it may still be possible that the glycopeptides are unable to undergo conformational changes which might be necessary for receptor binding. Glycosylated DDAVP analogues with retained antidiuretic activity and increased bioavailability might potentially be obtained by choosing another position for the carbohydrate moiety. Alternatively, glycosylated prodrugs of DDAVP can be envisaged, from which the carbohydrate is removed enzymatically in the plasma after absorption from the intestine. We would also like to emphasize that the conclusions presented in this paper could not have been drawn from either the pharmacological properties or the conformational studies alone.

Experimental Section

General. TLC was performed on Silica Gel 60 F_{254} (Merck) with detection by UV light and charring with sulfuric acid. Optical rotations were measured with a Perkin-Elmer 141 polarimeter. The ^1H NMR spectrum for **3** was recorded in $CDCl_3$ [residual $CHCl_3$ (δ_H 7.26) as internal standard] with a Varian XL-300 spectrometer. Positive fast atom bombardment mass spectra (FABMS) were recorded on a JEOL SX 102 A mass spectrometer. Ions were produced by a beam of Xenon atoms (6 keV) from a matrix of glycerol and thioglycerol. In the amino acid analyses, asparagine and glutamine were determined as aspartic acid and glutamic acid, respectively.

N^{α}-(9-Fluorenylmethoxycarbonyl)-L-serine pentafluorophenyl ester[16] (**2**) was prepared according to the indicated

literature method. [1-Desamino,8-D-arginine]vasopressin (DDAVP, **4**) was obtained from FERRING Research Institute AB (Sweden). Human serum albumin was from Behring (Germany). [^{3}H]PEG 1000 and [^{14}C]PEG 4000 were purchased from New England Nuclear (USA), and ^{125}I was from Amersham (England). Human plasma was obtained from Malmö General Hospital (Sweden). Bovine α-chymotrypsin was from Sigma (USA), and charcoal was obtained from Merck (Germany).

N^{α}-(9-Fluorenylmethoxycarbonyl)-3-*O*-(2,3,4,6-tetra-*O*-acetyl-β-D-galactopyranosyl)-L-serine Pentafluorophenyl Ester (3). Boron trifluoride etherate (310 μL, 2.5 mmol) was added to a solution of 1,2,3,4,5-penta-*O*-acetyl-β-D-galactopyranose (**1**, 390 mg, 1.0 mmol) and **2**[16] (420 mg, 0.85 mmol) in dry dichloromethane (11 mL) at room temperature. After 2.5 h the solution was washed with water (12 mL) and the aqueous phase was then extracted with dichloromethane (12 mL). The combined organic phases were dried (Na_2SO_4) and concentrated. Flash column chromatography (toluene–ethyl acetate, 6:1) of the residue on dry silica gel (Grace Amicon, 35–70 μm) gave **3** (297 mg, 42%) as a colorless amorphous solid: $[\alpha]^{25}_D$ −8.9° (*c* 0.95, chloroform); NMR ($CDCl_3$) δ 5.73 (1H, d, *J* = 8.4 Hz, NH), 5.39 (1H, bd, *J* = 2.5 Hz, H-4), 5.19 (1H, dd, *J* = 7.9 and 8.0 Hz, H-2), 5.05 (1H, dd, *J* = 8.0 and 2.5 Hz, H-3), 4.86 (1H, m, Ser-Hα), 4.50 (1H, d, *J* = 7.9 Hz, H-1), 4.44 (1H, m, Ser-Hβ), 4.11 (2H, d, *J* = 6.3 Hz, H-6,6′), 4.02 (1H, dd, *J* = 10.4 and 3.2 Hz, Ser-Hβ), 3.87 (1H, t, *J* = 6.4 Hz, H-5). Anal. ($C_{38}H_{34}NO_{14}F_5$) C, H, N.

General Procedure for Solid Phase Peptide Synthesis. The peptides **5**–**7** were synthesized using DMF as solvent in a mechanically agitated reactor. For each peptide, 0.25 g (0.4 mequiv/g, 100 μmol) of an aminomethylated polystyrene resin from Novabiochem (Switzerland), functionalized with the linker [*p*-[α-[(9-fluorenylmethoxy)formamido]-2,4-dimethoxybenzyl]phenoxy]acetic acid,[17,18] was used. Reagent solutions and DMF for washing were added manually to the reactor. N^{α}-Fmoc amino acids from Bachem (Switzerland) with the following protective groups were used: (2,2,5,7,8-pentamethylchroman-6-yl)sulfonyl (Pmc) for D-Arg, triphenylmethyl (Trt) for Asn, Cys, Gln, and 3-mercaptopropionic acid, and *tert*-butyl (tBu) for D-Tyr.

The N^{α}-Fmoc amino acids and mercaptopropionic acid were coupled to the peptide-resins as 1-benzotriazolyl (HOBt) esters.[19] These were prepared, *in situ*, from the appropriate acid (0.30 mmol), HOBt (61 mg, 0.45 mmol), and 1,3-diisopropylcarbodiimide (45 μL, 0.29 mmol) in DMF (1 mL). After 30–60 min the solution was added to the reactor. The glycosylated pentafluorophenyl ester **3** (165 mg, 0.20 mmol) was coupled in DMF (1 mL) containing HOBt (61 mg, 0.45 mmol). Acylations were monitored by addition of bromophenol blue[33] (0.05% of the resin capacity) to the reactor and by the ninhydrin test[34]. N^{α}-Fmoc deprotection was performed by treatment with 20% piperidine in DMF (2 + 8 min) or with 50% morpholine in DMF (2 + 2 × 15 min) after incorporation of **3** in the peptide.

After completion of the synthesis, the resin was washed with dichloromethane (5 × 5 mL) and dried under vacuum. The peptide (100 μmol) was then cleaved from the resin, and the amino acid side chains were deprotected by treatment with trifluoroacetic acid–water–thioanisole–ethanedithiol (87.5:5:5:2.5, 25 mL) for 2–3 h, followed by filtration. Acetic acid (15 mL) was added to the filtrate, the solution was concentrated, and the crude peptide solidified on trituration with diethyl ether (2 × 10 mL). The diethyl ether solutions were decanted, and the crude peptide was dried, dissolved in acetic acid–water (1:1), diluted with water, and freeze-dried.

Deacetylation of the carbohydrate moiety was achieved by stirring the crude glycopeptide in saturated methanolic ammonia (1.5 mL/mg glycopeptide) at room temperature for 3 h, followed by concentration.

Cyclization was performed immediately by alternating additions of portions of the crude peptide in acetic acid and 0.1 M I_2 in methanol to 10% acetic acid in methanol (2 mL/mg cleaved resin). After the final addition of I_2 a light brown solution was obtained which was neutralized and decolorized by stirring with Dowex 2 × 8 anion exchange resin (converted into acetate form by washing with 1 M aqueous NaOH, water, acetic acid, water, and methanol), filtered, and concentrated. The residue was then dissolved in water and freeze-dried.

Preparative HPLC separations were performed on a Beckman System Gold HPLC using a Kromasil C-8 column (1000 Å, 20 × 250 mm) with a flow rate of 12 mL/min and detection at 214 nm. Solvent systems: A, 0.1% aqueous trifluoroacetic acid and B, 0.1% trifluoroacetic acid in acetonitrile.

[Mpr^1,D-Tyr^2,Ser^4,D-Arg^8]vasopressin (5). Synthesis, cleavage of the resin-bound glycopeptide (25 μmol), cyclization, and purification by HPLC (20 % B in A, retention time: 22 min), according to the general procedure, gave **5** (11.3 mg, 44%): FABMS (M + H)$^+$ 1028 (calcd 1028). Amino acid analysis: Asp 1.00 (1), Arg 1.01 (1), Cys 0.98 (1), Gly 0.98 (1), Phe 1.02 (1), Pro 1.02 (1), Ser 1.02 (1), Tyr 0.98 (1).

[Mpr^1,D-Tyr^2,Ac$_4$-β-D-Galp-Ser^4,D-Arg^8]vasopressin (6). Synthesis, cleavage of the resin-bound glycopeptide (18 μmol), cyclization, and purification by HPLC (30% B in A, retention time: 17 min), according to the general procedure, gave **6** (7.3 mg, 30%): FABMS (M + H)$^+$ 1358 (calcd 1358). Amino acid analysis: Asp 1.01 (1), Arg 1.01 (1), Cys 0.96 (1), Gly 1.00 (1), Phe 1.01 (1), Pro 1.00 (1), Ser 1.00 (1), Tyr 1.01 (1).

[Mpr^1,D-Tyr^2,β-D-Galp-Ser^4,D-Arg^8]vasopressin (7). Synthesis, cleavage of the resin-bound glycopeptide (28 μmol), deacetylation, cyclization, and purification by HPLC (17% B in A, retention time: 40 min), according to the general procedure, gave **7** (6.7 mg, 20%): FABMS (M + H)$^+$ 1190 (calcd 1190). Amino acid analysis: Asp 1.00 (1), Arg 1.00 (1), Cys 0.97 (1), Gly 1.00 (1), Phe 1.01 (1), Pro 1.01 (1), Ser 1.01 (1), Tyr 0.99 (1).

Degradation with α-Chymotrypsin and Rat Intestinal Juice. Degradation of the peptides **4**–**7** by α-chymotrypsin was performed by incubating peptide (1 mM final concentration) and α-chymotrypsin (1 mg/mL final concentration) at 37 °C in buffer (25 mM Tris, 65 mM NaCl, 2.5 mM $CaCl_2$, pH 7.8, 30 μL final volume). The degradation was arrested by addition of ice cold aqueous trichloroacetic acid (12.5%, 20 μL), after which the sample was centrifuged (10000*g*, 5 min, 4 °C). The time-course of the degradation was determined by analyzing the peptide content in the supernatant of the centrifuged samples by reversed-phase HPLC. The peptide content was obtained by comparison of the peak area of each sample with a reference sample treated in the same way, but with omission of enzyme in the incubation.

Rat intestinal juice was obtained by rinsing a 10 cm segment of small intestine with 5 mL of 0.9% NaCl. After centrifugation at 10000*g* for 15 min, the supernatant of the rat intestinal juice preparation was immediately frozen in small portions at −20 °C. Since there was a slight batch-to-batch variation in the degradative activity of the rat intestinal juice, it was normalized using DDAVP as standard.

Degradation by rat intestinal juice was studied in the same way as with chymotrypsin, except that the Tris concentration was 165 mM. The amount of the intestinal juice preparation added was chosen to give a degradation rate of DDAVP of 2%/min. It was verified that the rat intestinal juice did not contain any endogenous peaks at the elution positions of the respective peptides.

Transport of Peptides *in Vitro* over Rat Small Intestine. The small intestine of a Sprague–Dawley rat (250–300 g) was dissected and immersed in oxygenated (carbogen; 95% O_2, 5% CO_2) Krebs-Ringer buffer, pH 7.4, at 0 °C. Three adjacent pieces of the intestine, approximately 35 cm distal to pylorus, were carefully cut out under the microscope in order to avoid the Peyer's patches. The pieces were rinsed with buffer, and care was taken not to damage the villi structures on the mucosal side. Each piece of intestine was then mounted on the inner tissue holding frame (basolateral chamber) of a modified Ussing chamber assembly, showing the mucosal side to the outer chamber (apical chamber). Buffer was added to exactly the same level in the apical and the basolateral chambers (13.5 and 1.0 mL, respectively), and both compartments were continuously oxygenated with carbogen. In all experiments with compounds **5**–**7**, a DDAVP experiment was run in parallel. The temperature was kept at 37 °C, and a constant, digitally controlled stirring rate was maintained in the apical chamber. The inner area of the basolateral chamber

was 1.47 cm^2 which is identical to the area of intestine available for transport. After equilibration, the peptide, [^{3}H]-PEG 1000 and [^{14}C]PEG 4000 were added to the apical chamber at final concentrations of 10, 20, (250 000 cpm/mL), and 4 μM (500 000 cpm/mL), respectively. Aliquots (600 μL) were withdrawn from the basolateral chamber for analysis at 15 min intervals and immediately replaced with fresh thermostated buffer. The aliquots were instantly frozen at −78 °C and kept frozen until analyzed by radioimmunoassay or liquid scintillation counting. It was verified that no degradation of the peptides occurred in the chambers during the experiment or during storage prior to analysis. The transport rate over the small intestine is expressed as P_{app} (cm/s), calculated according to the formula

$$P_{app} = (dQ/dt)/(AC_0)$$

where dQ/dt is the actual transport rate (mol/s), C_0 is the initial concentration in the apical chamber (mol/mL), and A is the area of intestine available for transport (cm^2).

Intravenous and Intraintestinal Administration of Peptides *in Vivo* in Rats. Male Sprague−Dawley rats (250−300 g) were anaesthetized with Inactin and kept at 37 °C on a thermostated heating plate. All solutions used in the experiments were prewarmed to 37 °C. A 15 cm intestinal segment beginning 10 cm distal to pylorus was opened and cannulated at each end using silicon tubing, and the segment was then gently rinsed with 0.9% NaCl (10 mL) in order to remove food remnants. After a recovery period of 30 min, the peptide (100 μg) was administered in 1 mL of 0.9% aqueous NaCl through the tubing. The intravenous administration was performed by injecting the peptide (1.0 μg) dissolved in 0.9% sterile aqueous NaCl (0.2 mL) into the previously catheterized vena jugularis. Blood samples (0.2 mL) were collected from the catheterized arteria carotis, EDTA plasma was prepared immediately, and the samples were kept frozen until analyzed by radioimmunoassay. The area under the plasma concentration curve (AUC) was calculated using the trapezoidal rule, and the bioavailability was calculated according to the formula $(AUC_{ii}/dose_{ii})/(AUC_{iv}/dose_{iv})$.

Radioimmunoassay. The concentration of peptide in the samples from the *in vitro* and *in vivo* assays was determined by radioimmunoassay using the antibody ADA 6, which was raised against the C-terminal part of DDAVP[35,36] Sample aliquots were analyzed, without prior extraction, in 400 μL of RIA-buffer (0.1 M Na-phosphate, pH 7.5, 50 mM NaCl, 0.1% human serum albumin, 0.02% NaN_3, 0.01% Triton X-100), containing ADA 6 (dilution 1:160 000) and 1−2 fmol tracer ([^{125}I]Tyr^2-DDAVP). After incubation over two nights at 4 °C, 0.5% charcoal in RIA-buffer supplemented with 2.5% human normal plasma was added to adsorb free tracer, and antibody bound tracer was determined in the supernatant after centrifugation. The antibody crossreacted by approximately 25% with the peptides **5**−**7**, and the lowest detectable amount of the peptides was approximately 1 pg per assay tube.

Agonistic and Antagonistic Properties of Peptides at the Vasopressin Receptor. The agonistic, i.e., the antidiuretic, activity was determined *in vivo* using overnight hydrated male Sprague−Dawley rats as described previously by others.[37] The antagonistic activity *in vivo* was also determined in this model. Increasing doses of the peptide were injected 1 min prior to the administration of a fixed dose of vasopressin. The vasopressin dose was chosen individually for each rat such that the antidiuretic response without antagonist was approximately the same for all rats.

The antagonistic properties *in vitro* were analyzed in a rat renal medullary membrane receptor assay.[38] Membrane protein (250 μg) was incubated for 120 min at room temperature with 1 nM [^{3}H]vasopressin and increasing concentrations of the peptide in the presence or absence of 10 nM of the potent and specific V_1-antagonist [Phenylac^1,D-Tyr(Me)^2,Arg^{6,8},Lys-NH_2^{9}]vasopressin (Bachem AG, Switzerland). The incubation was terminated by pelleting the membrane fraction, and after several washes the [^{3}H]vasopressin bound to the membrane fraction was analyzed by liquid scintillation counting.

^{1}H NMR Spectroscopy. Compounds **4**, **6**, and **7** were dissolved in 9:1 mixtures of H_2O and D_2O at concentrations of 13, 5.4, and 6.4 mM. Samples of **4**, **6**, and **7** in D_2O were also prepared at concentrations of 13, 5, and 6 mM. For all samples pH was adjusted to 5.65 with solutions of 0.4% NaOD and 0.4% DCl in D_2O.

^{1}H NMR spectra were collected at 500.13 MHz on a General Electric Omega 500 spectrometer. Phase-sensitive COSY,[39] TOCSY,[40] and ROESY[41] spectra were recorded at 5 °C using the water resonance at 4.98 ppm as internal shift reference. All ROESY spectra were acquired with a mixing period of 200 ms, except the ROESY spectrum for the D_2O sample of **4**, where 300 ms was used. The acquired data were processed with the Felix software (Biosym Technologies, USA). Complete assignment of all proton resonances, with the exception of Cys^6 H-α in **6** which was to close to the water resonance, was achieved using standard methods.[42] A more detailed description of the NMR experiments is given in ref 21.

Interproton cross peaks from the ROESY spectra were volume integrated and interproton distances, d_{ij}, were calculated according to the relation

$$d_{ij} = d_{ref}(V_{ref}/V_{ij})^{1/6}$$

in which d_{ref} stands for a known interproton distance between two reference protons, and V_{ij} and V_{ref} stand for the integrated volumes of cross peak ij and the cross peak between the reference protons. The geminal β-protons in Phe^3 were used as reference protons (interproton distance: 1.78 Å) in the spectra for **4**, **6**, and **7**. The three dimensional structures were generated with distance geometry calculations and simulated annealing using the software X-PLOR.[43]

Acknowledgment. Skilful technical assistance was provided by Mrs. Maria Abbe-Nilsson, Mrs. Birgitta Andersson, Mrs. Elisabeth Bergman, Ms. Cecilia Hansson, Mrs. Karin Hansson, Mr. Anders Nylén, and Ms. Agnes Sokolnicka. The RIA-group of Ferring AB is acknowledged for providing the tracer. This work was funded in part by the Swedish National Board for Industrial and Technical Development, the Swedish Medical Research Council, and Crafoordska Stiftelsen.

References

(1) Varki, A. Biological Roles of Oligosaccharides: All of the Theories are Correct. *Glycobiology* **1993**, *3*, 97−130.
(2) Lis, H.; Sharon, N. Protein Glycosylation: Structural and Functional Aspects. *Eur. J. Biochem.* **1993**, *218*, 1−27.
(3) Fisher, J. F.; Harrison, A. W.; Bundy, G. L.; Wilkinson, K. F.; Rush, B. D.; Ruwart, M. J. Peptide to Glycopeptide: Glycosylated Oligopeptide Renin Inhibitors with Attenuated in Vivo Clearance Properties. *J. Med. Chem.* **1991**, *34*, 3140−3143.
(4) Rodriguez, R. E.; Rodriguez, F. D.; Sacristán, M. P.; Torres, J. L.; Valencia, G.; Garcia Antón, J. M. New Glycosylpeptides with High Antinociceptive Activity. *Neurosci. Lett.* **1989**, *101*, 89−94.
(5) Polt, R.; Porecca, F.; Szabò, L.; Hruby, V. J. Synthesis of Glycosyl-Enkephalin Analogues which Rapidly Cross the Blood-Brain Barrier to Produce Analgesia in Mice. An Entirely New Class of "Designer Drugs". *Glycoconj. J.* **1993**, *10*, 261.
(6) Bardaji, E.; Torres, J. L.; Clapés, P.; Albericio, F.; Barany, G.; Rodriguez, R. E.; Sacristán, M. P.; Valencia, G. Synthesis and Biological Activity of *O*-Glycosylated Morphiceptin Analogues. *J. Chem. Soc., Perkin Trans. 1* **1991**, 1755−1759.
(7) Varga-Defterdarovic, L.; Horvat, S.; Chung, N. N.; Schiller, P. W. Glycoconjugates of Opioid Peptides. *Int. J. Pept. Protein Res.* **1992**, *39*, 12−17.
(8) Lavielle, S.; Ling, N.; Brazeau, P.; Benoit, R.; Wasada, T.; Harris, D.; Unger, R.; Guillemin, R. Synthesis and Biological Activity of Glycosylated Analogues of Somatostatin. *Biochem. Biophys. Res. Commun.* **1979**, *91*, 614−622.
(9) Geiger, R.; Köning, W.; Sandow, J. Design and Synthesis of Hypothalamic Hormone Analogues. In *Peptides: Chemistry, Biology, Interactions with Proteins*; Penke, B., Török, A., Eds.; Proceedings of the 50th Anniversary Symposium of the Nobel-Prize of Albert Szent-Györgi; Walter de Gruyter & Co.: Berlin, 1988; pp 385−392.
(10) Gobbo, M.; Biondi, L.; Filira, F.; Scolaro, B.; Rocchi, R.; Piek, T. Synthesis and Biological Activity of the Mono- and Di-Galactosyl-Vespulakinin 1 Analogues. *Int. J. Pept. Protein Res.* **1992**, *40*, 54−61.

(11) Plattner, J. J.; Norbeck, D. W. Obstacles to Drug Development from Peptide Leads. In *Drug Discovery Technologies*; Clark, C. R., Moos, W. R., Eds.; Ellis Harwood Ltd.–Halstead Press: Chichester, England, 1989; pp 92–126.
(12) Powell, M. F.; Stewart, T.; Otvos, L., Jr.; Urge, L.; Gaeta, F. C. A.; Sette, A.; Arrhenius, T.; Thomson, D.; Soda, K.; Colon, S. M. Peptide Stability in Drug Development. II. Effect of Single Amino Acid Substitution and Glycosylation on Peptide Reactivity in Human Serum. *Pharm. Res.* **1993**, *10*, 1268–1273.
(13) Zaoral, M. Vasopressin Analogs with High and Specific Antidiuretic Activity. *Int. J. Pept. Protein Res.* **1985**, *25*, 561–574.
(14) Hruby, V. J.; Smith, C. W. Structure-Activity Relationships of Neurohypophyseal Peptides. In *The Peptides; Analysis, Synthesis, Biology*, vol. 8, *Chemistry, Biology, and Medicine of Neurohypophyseal Hormones and Their Analogs*; Smith, C. W., Ed.; Academic Press, Inc.: Orlando, 1987; pp 179–188.
(15) Magnusson, G.; Noori, G.; Dahmén, J.; Frejd, T.; Lave, T. BF_3 - Etherate Induced Formation of 2,2,2-Trichloroethyl Glycopyranosides. Selective Visualization of Carbohydrate Derivatives on TLC Plates. *Acta Chem. Scand., Ser. B* **1981**, *35*, 213–216.
(16) Kisfaludy, L.; Schön, I. Preparation and Applications of Pentafluorophenyl Esters of 9-Fluorenylmethyloxycarbonyl Amino Acids for Peptide Synthesis. *Synthesis* **1983**, 325–327.
(17) Rink, H. Solid-Phase Synthesis of Protected Peptide Fragments Using a Trialkoxy-Diphenyl-Methylester Resin. *Tetrahedron Lett.* **1987**, *28*, 3787–3790.
(18) Bernatowicz, M. S.; Daniels, S. B.; Köster, H. A Comparison of Acid Labile Linkage Agents for the Synthesis of Peptide C-Terminal Amides. *Tetrahedron Lett.* **1989**, *30*, 4645–4648.
(19) König, W.; Geiger, R. Eine neue Methode zur Synthese von Peptiden: Aktivierung der Carboxylgruppe mit Dicyclohexylcarbodiimid unter Zusatz von 1-Hydroxy-benzotriazolen. (New method for the synthesis of peptides: Activation of the carboxyl group with dicyclohexylcarbodiimide by using 1-hydroxybenzotriazoles as additives.) *Chem. Ber.* **1970**, *103*, 788–798.
(20) Fjellestad-Paulsen, A.; Höglund, P.; Lundin, S.; Paulsen, O. Pharmacokinetics of 1-Deamino-8-D-arginine Vasopressin after Various Routes of Administration in Healthy Volunteers. *Clin. Endocrinol.* **1993**, *38*, 177–182.
(21) Walse, B.; Kihlberg, J.; Drakenberg, T. Conformation of the Vasopressin Analogue DDAVP in Aqueous Solution. Manuscript in preparation.
(22) Langs, D. A.; Smith, G. D.; Stezowski, J. J.; Hughes, R. E. Structure of Pressinoic Acid: The Cyclic Moiety of Vasopressin. *Science* **1986**, *232*, 1240–1242.
(23) Hempel, J. C. The Conformation of Neurohypophyseal Hormones. In *The Peptides; Analysis, Synthesis, Biology*, vol. 8, *Chemistry, Biology, and Medicine of Neurohypophyseal Hormones and Their Analogs*; Smith, C. W., Ed.; Academic Press, Inc.: Orlando, 1987; pp 209–237.
(24) Schmidt, J. M.; Ohlenschläger, O.; Rüterjans, H.; Grzonka, Z.; Kojro, E.; Pavo, I.; Fahrenholz, F. Conformation of [8-Arginine]-vasopressin and V_1 Antagonists in Dimethyl Sulfoxide Solution Derived from Two-Dimensional NMR Spectroscopy and Molecular Dynamics Simulation. *Eur. J. Biochem.* **1991**, *201*, 355–371.
(25) Elofsson, M.; Roy, S.; Walse, B.; Kihlberg, J. Solid-Phase Synthesis and Conformational Studies of Glycosylated Derivatives of Helper-T-Cell Immunogenic Peptides from Hen-Egg Lysozyme. *Carbohydr. Res.* **1993**, *246*, 89–103.
(26) Jansson, A. M.; Meldal, M.; Bock, K. Solid-Phase Synthesis and Characterization of *O*-Dimannosylated Heptadecapeptide Analogues of Human Insulin-like Growth Factor 1 (IGF-1). *J. Chem. Soc., Perkin Trans. 1* **1992**, 1699–1707.
(27) Delbaere, L. T. J.; Vandonselaar, M.; Prasad, L.; Quail, J. W.; Pearlstone, J. R.; Carpenter, M. R.; Smillie, L. B.; Nikrad, P. V.; Spohr, U.; Lemieux, R. U. Molecular Recognition of a Human Blood Group Determinant by a Plant Lectin. *Can. J. Chem.* **1990**, *68*, 1116–1121.
(28) Cygler, M.; Rose, D. R.; Bundle, D. R. Recognition of a Cell-Surface Oligosaccharide of Pathogenic *Salmonella* by an Antibody Fab Fragment. *Science* **1991**, *253*, 442–445.
(29) Gerz, M.; Matter, H.; Kessler, H. Synthesis and Solution Structure of an S-glycosylated Cyclic Hexapeptide. *Int. J. Pept. Protein Res.* **1994**, *43*, 248–257.
(30) Urge, L.; Jackson, D. C.; Gorbics, L., Wroblewski, K.; Graczyk, G.; Otvos, L., Jr. Synthesis and Conformational Analysis of N-glycopeptides that Contain Extended Sugar Chains. *Tetrahedron* **1994**, *50*, 2373–2390.
(31) Andreotti, A. H.; Kahne, D. Effects of Glycosylation on Peptide Backbone Conformation. *J. Am. Chem. Soc.* **1993**, *115*, 3352–3353.
(32) Otvos, L., Jr.; Thurin, J.; Kollat, E.; Urge, L.; Mantsch, H. H.; Hollosi, M. Glycosylation of Synthetic Peptides Breaks Helices. *Int. J. Pept. Protein Res.* **1991**, *38*, 476–482.
(33) Flegel, M.; Sheppard, R. C. A Sensitive, General Method for Quantitative Monitoring of Continuous Flow Solid Phase Peptide Synthesis. *J. Chem. Soc., Chem. Commun.* **1990**, 536–538.
(34) Kaiser, E.; Colescott, R. L.; Bossinger, C. D.; Cook, P. I. Color Test for Detection of Free Terminal Amino Groups in the Solid-Phase Synthesis of Peptides. *Anal. Biochem.* **1970**, *34*, 595–598.
(35) Lundin, S.; Melin, P.; Vilhardt, H. Plasma Concentration of 1-Deamino-8-D-arginine Vasopressin after Intragastric Administration in the Rat. *Acta Endocrinol.* **1985**, *108*, 179–183.
(36) Jönsson, K.; Alfredsson, K.; Söderberg-Ahlm, C.; Critchley, H.; Broeders, A.; Ohlin, M. Evaluation of the Degradation of Desamino[1], D-arginine[8]-vasopressin by Nasal Mucosa. *Acta Endocrinol.* **1992**, *127*, 27–32.
(37) Larsson, L.-E.; Lindeberg, G.; Melin, P.; Pliska, V. Synthesis of O-Alkylated Lysine-vasopressins, Inhibitors of the Antidiuretic Response to Lysine-vasopressin. *J. Med. Chem.* **1978**, *21*, 352–356.
(38) Marchingo, A. J.; Abrahams, J. M.; Woodcock, E. A.; Smith, A. I.; Mendelsohn, F. A. O.; Johnston, C. I. Properties of [^{3}H]1-Desamino-8-D-Arginine Vasopressin as a Radioligand for Vasopressin V_2-Receptors in Rat Kidney. *Endocrinology* **1988**, *122*, 1328–1336.
(39) Aue, W. P.; Bartholdi, E.; Ernst, R. R. Two-dimensional Spectroscopy. Application to Nuclear Magnetic Resonance. *J. Chem. Phys.* **1976**, *64*, 2229–2246.
(40) Braunschweiler, L.; Ernst, R. R. Coherence Transfer by Isotropic Mixing: Application to Proton Correlation Spectroscopy. *J. Magn. Reson.* **1983**, *53*, 521–528.
(41) Bax, A.; Davis, D. G. Practical Aspects of Two-Dimensional Transverse NOE Spectroscopy *J. Magn. Reson.* **1985**, *63*, 207–213.
(42) Wüthrich, K. *NMR of Proteins and Nucleic Acids*; Wiley: New York, 1986.
(43) Brünger, A. T. *X-PLOR, Version 3.1. A System for X-Ray Crystallography and NMR*; Yale University Press: New Haven, 1992.

JM940458+